Cellular Physiology and Biochemistry

Cell Physiol Biochem 2016;38:1063-1074
DOI: 10.1159/000443057
Published online: March 04, 2016
Accepted: January 08, 2016

1421-9778/16/0383-1063$39.50/0

Original Paper

Oxygen-Glucose-Deprivation / Reoxygenation-Induced Autophagic Cell Death Depends on JNK-Mediated Phosphorylation of Bcl-2

Jin Fan[a] Yuwen Liu[b] Jian Yin[a] Qingqing Li[a] Yiming Li[c] Jun Gu[d] Weihua Cai[a] Guoyong Yin[a]

[a]Department of Orthopaedics, The First Affiliated Hospital of Nanjing Medical University, Nanjing, [b]Department of Orthopaedics, Nanjing Children's Hospital, Nanjing, [c]Department of Orthopaedics, Xuzhou Central Hospital, Xuzhou, [d]Xi Shan People's Hospital, WuXi, China

Key Words
Autophagic cell death • Bcl-2 • JNK • Neuron

Abstract
Background/Aims: The purpose of this study was to investigate the role of autophagy in oxygen-glucose-deprivation/reoxygenation (OGD/R) injury in rat neurons***. Methods and results:*** Cortical neurons were isolated from Sprague-Dawley rats and identified by immunofluorescence. The cortical neurons were randomly assigned to one of four groups: control group (I), experimental group (OGD/R group, II), JNK inhibitor pretreatment group (III) and JNK inhibitor pretreatment + OGD/R group (IV). Neuronal cell viability significantly decreased after 6h and 12h of reoxygenation in Group IV ($P < 0.05$). Electron microscopy showed the presence of many autophagic vacuoles and the formation of autolysosomes in the neurons; the number of autophagic vacuoles decreased transiently at 6h, while a new autophagic flux and a large number of empty autophagic vacuoles were observed at 12h. In Group IV, a large number of autophagic vacuoles were present at 0.5h and 2h of reoxygenation, which gradually decreased with increasing reoxygenation time. No significant differences in the expression of the LC3II protein were detected between the Group II and IV prior to 6h of reoxygenation, and LC3II expression showed an overall rise-decline pattern. However, LC3II protein expression increased in Group II at 12h of reoxygenation, whereas a continuous decline was observed in Group IV. The levels of phosphorylated JNK and Bcl-2 and the expression of Beclin-1 increased gradually as the reoxygenation time going in Group II, whereas they increased at 12h of reoxygenation in Group IV ($P < 0.05$). In addition, progressive dissociation of the Bcl-2/Beclin-1 complex was observed in the Group II, while JNK inhibitor suppressed this dissociation. ***Conclusion:*** The regulation of the JNK/Bcl-2/Beclin-1 signaling pathway may be one of the mechanisms underlying the OGD/R-induced autophagic cell death of neurons.

J. Fan and Y. Liu contributed equally to this work.

Guoyong Yin and Weihua Cai
Department of Orthopaedics, The First Affiliated Hospital of Nanjing Medical University, Jiangsu 210029, (China)
E-Mail guoyong_yin@sina.com, E-Mail caiwhspine@sina.com

Introduction

Macroautophagy (hereafter called autophagy) is a form of cellular self-cannibalism in which organelles and proteins are degraded into simple components, such as the degradation of proteins to amino acids and nucleic acids to nucleotides. In autophagy, the recycling and reuse of macromolecules plays a critical role in maintaining cellular energy levels and promoting cell survival [1]. Autophagy operates at a low basal level under physiological conditions; however, it plays important roles in the adaptation of cells to the external environment [2]. Autophagy can be activated by strong extracellular stimuli such as starvation, viral infections, ischemia and hypoxia [3]; however, excessive activation of the autophagic pathway results in the attack and phagocytosis of normal organelles leading to autophagic cell death (also called type II cell death) [4]. Autophagic cell death lacks the classic features of apoptosis such as nuclear pyknosis and chromosome aggregation, and is characterized by the formation of specific single- or double-membrane structures such as phagophores, autophagic vacuoles and autolysosomes [5].

Microtubule-associated protein 1 light chain 3 (LC3), a mammalian homologue of the yeast ATG8 gene (Aut7/Apg8), is located on the surface of pre-autophagic vacuoles and the autophagic vacuole membrane. LC3 is a universal marker of autophagosomes because it does not bind to other vesicular structures [6]. LC3 exists in two forms: LC3I (cytosol) and LC3II (membrane bound). LC3 precursors (ProLC3) are proteolytically processed to form LC3I, which is converted to LC3II by sumoylation [7]. In addition, the level of LC3-II therefore reflects autophagic activity in cells to some extent [8].

Beclin-1, a mammalian protein involved in autophagy, is an orthologue of the yeast autophagy protein Apg6/Vps30. Although Beclin-1 is not directly involved in autophagic vacuole formation, the upregulation of Beclin-1 expression activates autophagy [7, 8]. Beclin-1 contains a conserved Bcl-2 homology 3 (BH3) domain similar to that of the Bcl-2 family of proteins; therefore, it is considered as a novel BH3-only member of the Bcl-2 protein family [9]. Beclin-1 can stably bind to other Bcl-2 family members via a hydrophobic groove on the BH3 domain, thereby mediating cellular physiological functions [9, 10]. Under normal physiological conditions, anti-apoptotic Bcl-2 proteins can stably bind to other pro-apoptotic proteins, thereby maintaining cellular homeostasis [11, 12]. Acute starvation induces phosphorylation of Bcl-2 at specific serine and threonine residues, resulting in its inactivation and dissociation from Beclin-1, which activates autophagy [13].

As members of the mitochondrial pathway of apoptosis, a classical apoptotic pathway, the activity of the Bcl-2-family proteins is often mediated by their upstream protein kinase, C-Jun N-terminal kinase (JNK) [14]. JNK is a type of serine/threonine kinase that belongs to the third mitogen-activated protein kinase (MAPK) family identified in mammals [15]. In our previous study, we showed that spinal cord ischemia-reperfusion injury activates JNK, resulting in the activation of the anti-apoptotic proteins of the Bcl-2 family and the induction of apoptosis of spinal neurocytes [16]. However, the involvement of the JNK signaling pathway in the regulation of neuronal viability by autophagy remains unclear. In current study, we characterized the mechanisms and function of autophagy in neurons following the Oxygen-glucose-deprivation/ reoxygenation.

Materials and Methods

Culture and identification of primary rat cortical neurons

Primary cortical neuronal cultures were prepared from embryonic 18-d-old fetal Sprague-Dawley rats using a method described previously [17]. Briefly, cerebral cortices were removed from 18-d-old embryonic rat fetuses under aseptic conditions, and dissociated using trypsin/DNase I for 20 min. Neurons were seeded at a density of 5×10^5 cells/cm^2 in 12-well culture plates pre-coated with poly-L-lysine, and maintained in fresh Neurobasal media containing 2% B27, 1% glutamine, 100 IU/ml penicillin and 100 mg/ml streptomycin. One half of the medium was changed every 3 days. After 7 days of cell culture *in vitro*,

neurons were identified by immunofluorescence with a specific antibody against microtubule-associated protein (MAP)-2.

Groups

All experiments were performed on cortical neuronal cultures 7 days after initial plating. The OGD/R model was established as described previously [18]. The cortical neurons were randomly assigned to one of four groups: Control group, Experimental group (OGD/R group), JNK inhibitor treatment group, and JNK inhibitor pretreatment + OGD/R group. The neurons in the blank control group were cultured in glucose-containing Dulbecco's modified Eagle's medium (DMEM) at 37°C in an incubator containing 5% CO_2. In the experimental group, the neurons were washed with glucose-free phosphate buffered saline (PBS) to remove the primary medium, and then incubated in 2 ml of glucose-free DMEM. Cells were placed in an anaerobic chamber aerated with an aerobic gas mix (95% N_2 and 5% CO_2) at 37°C for 30 min to reduce the oxygen content to less than 1%. The chamber was sealed, and the medium was replaced with glucose-containing DMEM. The neurons were immediately transferred to an incubator containing 5% CO_2 and cultured for 0.5 h, 2 h, 6 h and 12 h at 37°C. Cells in the JNK inhibitor treatment group were maintained in glucose-containing DMEM in an incubator containing 5% CO_2 at 37°C. When the neurons reached maturity, the medium was supplemented with 10μmol/L SP600125 (Sigma-Aldrich, St. Louis, MO, USA) dissolved in dimethyl sulfoxide (DMSO). After 0.5 h, the medium was replaced with normal DMEM for a further culture of 0.5, 2, 6 and 12 h. In the JNK inhibitor pretreatment + OGD/R group, the neurons were maintained in medium supplemented with 10 μmol/L SP600125 dissolved in DMSO 0.5 h prior to the OGD/R [19]; experimental procedures and subgrouping were performed as described for the experimental group.

Neuronal viability assessment by the 3-(4, 5-dimethylthiazol-2-yl) -2, 5-diphenyl tetrazolium bromide (MTT) assay

Neuronal viability was assessed by measuring the activity of mitochondrial dehydrogenase (MDH) using the MTT assay (Gibco; Gaithersburg, MD, USA). Survival of neurons in the blank control group was defined as 100% and the results were expressed as percentage relative to the control values [20].

Western blot analysis

Cultured neurons were harvested, lysed with RIPA lysis buffer (Beyotime Institute of Biotechnology, Songjiang, Shanghai, China), and protein was extracted. Protein concentration was determined using the Bradford method. Equal amounts of protein were separated by sodium dodecyl sulfate polyacrylamide gel electrophoresis (SDS-PAGE) and transferred to polyvinylidene difluoride (PVDF) membranes (Millipore, Billerica, MA, USA). PVDF membranes were incubated with the corresponding primary antibodies at 4°C overnight, and then with horseradish peroxidase (HRP)-conjugated secondary antibodies (Beyotime Institute of Biotechnology, Songjiang, Shanghai, China) at 37°C for 2 h. Reacting bands were visualized using enhanced chemiluminescence (ECL) reagents (Beyotime Institute of Biotechnology; Songjiang, Shanghai, China), and the density of the protein bands was quantified using the software Quantity One.

Immunofluorescence assay

Neurons were cultured for the indicated times, the medium was removed and cells were washed twice with pre-cooled PBS, fixed in 4% paraformaldehyde for 15 min, and then washed twice with PBS. Neurons were then permeabilized with 0.1% Triton-X 100 for 30 min, washed twice with PBS, blocked in blocking buffer containing 2% skimmed milk at room temperature for 1 h, and washed twice with PBS. Neurons were incubated in primary antibody diluted with blocking buffer at 4°C overnight. On the following day, cells were washed three times with PBS, and then incubated in Cy3- or FITC-conjugated secondary antibodies (Beyotime Institute of Biotechnology, Songjiang, Shanghai, China) at room temperature in the dark for 2 h. Subsequently, the neurons were washed three times with PBS, dehydrated through a 50%, 70%, 95%, and 100% ethanol graded series, treated with fluorescence mounting medium, and overlapped on anhydrous ethanol-treated slides. The slides were dried in room air, and visualized under a fluorescence microscope.

Beclin-1/Bcl-2 co-immunoprecipitation assay

The neurons in each group were lysed and centrifuged, and a 500-μg aliquot of each supernatant was treated with 3 μl of anti-Bcl-2 antibody (Abcam; Cambridge, UK) and shaken gently at 4°C overnight, then

shaken gently at 4°C for 2 h after the addition of 30 µl of Protein G/Protein A agarose beads (Calbiochem; San Diego, CA, USA). Samples were centrifuged at 4000 revs/min at 4°C for 3 min and the supernatant was removed. The neurons were washed three times, treated with 6 µl of loading buffer and boiled for 5 min. The supernatants were analyzed by protein electrophoresis. The determination of Bcl-2 and Beclin-1 concentrations was performed as described in Western blot analysis.

Statistical analysis

All data were expressed as mean ± standard deviation (SD), and all experiments were repeated independently three times. Student's t-test or one-way analysis of variance (ANOVA) was used to analyze differences between groups. A *P*-value < 0.05 was considered statistically significant.

Results

Identification of cortical neurons

Cultured cells isolated from Sprague-Dawley rats stained positive for MAP-2 by immunofluorescence, confirming their identity as cortical neurons with a purity > 90% (Fig. 1).

Neuronal viability assessment by the MTT assay

Neuronal viability was slightly lower in the JNK inhibitor treated group than in the blank control group, reflecting the effect of the JNK inhibitor on neurons ($P > 0.05$). Neuronal viability showed a tendency to decrease gradually with increasing reoxygenation time in the experimental group and the JNK inhibitor pretreatment + OGD/R group, with a more notable reduction in the experimental group ($P < 0.05$). Neuronal viability decreased significantly in the experimental group at 6 and 12 h of reoxygenation, with relative survival rates of 29% and 13%, respectively, while these values were 56% and 41% in the JNK inhibitor pretreatment + OGD/R group (Fig. 2). These results indicated that OGD/R caused significant damage to neurons and pretreatment with JNK inhibitors suppressed this effect.

Electron microscopic observation

The neuronal soma was plump and showed normal morphology in the control group, with intact nuclear and plasma membranes and normal aggregation of organelles including mitochondria and endoplasmic reticulum. No damage such as fragment-like dispersion or swelling was observed. A large number of crescent-shaped or goblet-like phagophores were observed in the experimental group after 0.5 h of reoxygenation; most of them had double- or multiple-layer membrane structures and contained cytoplasmic components. After 2 h of reoxygenation, autophagosomes with double- or multiple-layer membrane structures containing cytoplasmic components or cell fractions were observed; organelles

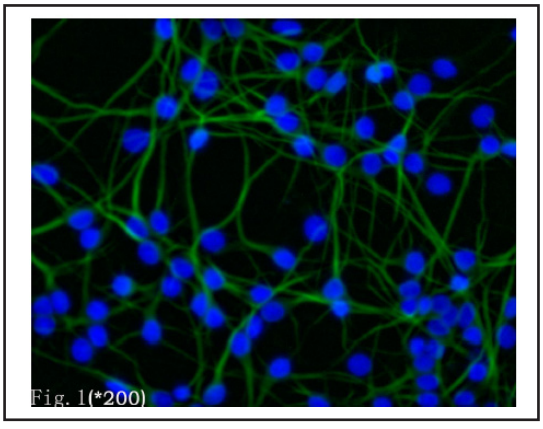

Fig. 1. Identification of cortical neurons by immunofluorescence with a specific antibody against MAP-2. The results showed that the percentage of cortical neuronal cultures reached 90% (*200).

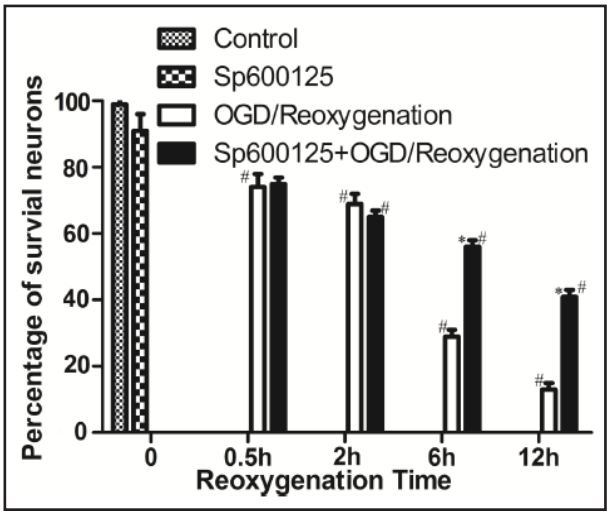

Fig. 2. Neuronal viability assessed with the MTT assay. Neuronal viability showed a gradual decrease with increasing reoxygenation time in the experimental group and the inhibitor pretreatment + oxygen-glucose-deprivation/reoxygenation (OGD/R) group, and a more notable reduction was observed in the experimental group than in the JNK inhibitor pretreatment + OGD/R group (# $P < 0.05$, experimental group vs. blank control group, and JNK inhibitor pretreatment + OGD/R group vs. JNK inhibitor treatment group; * $P < 0.05$, JNK inhibitor pretreatment + OGD/R group vs. experimental group).

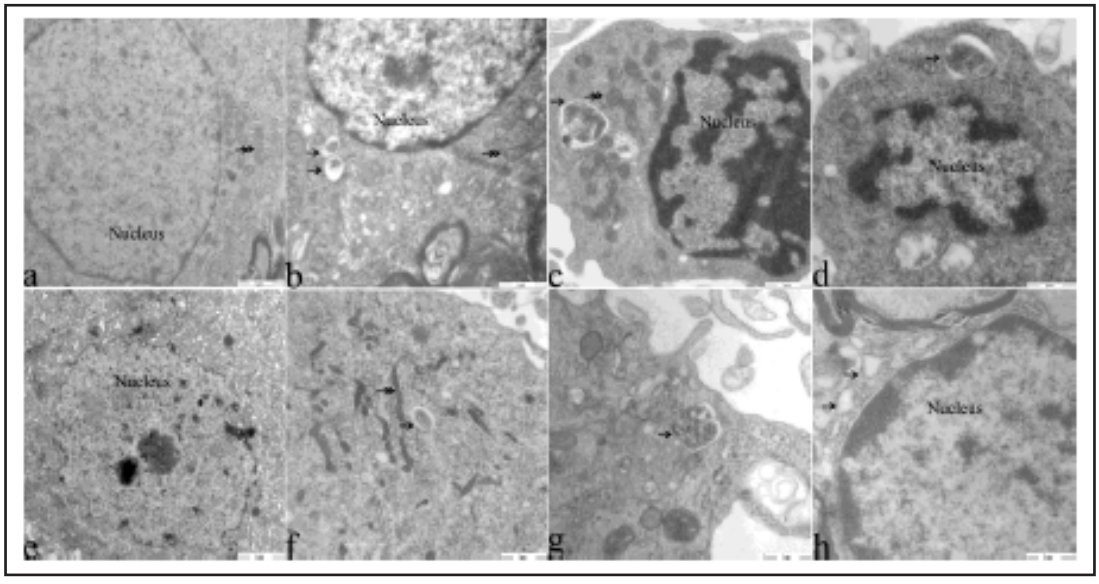

Fig. 3. Electron microscopic analysis of autophagosome formation. (a) The neuronal soma is plump and shows a normal morphology, with intact nuclear and plasma membranes. (b) At 0.5 and 2h of reoxygenation, crescent-shaped or goblet-like phagophores with double- or multiple-layer membrane structures and formation of autophagosomes is observed in the experimental group. (C) After 6 h of reoxygenation, autophagic vacuoles fused with lysosomes to form autolysosomes with single-layer membrane structures in the experimental group. (d) A large number of newly formed lysosomes is observed in the experimental group after 12 h of reoxygenation. (e) The neuronal soma is not very plump in the JNK inhibitor treatment group, with shrinking of the nuclear and plasma membranes; no cellular damage is observed (Data was not shown). (f) The morphology of mitochondria and the endoplasmic reticulum remains intact, without apparent swelling or rupture in the JNK inhibitor pretreatment + oxygen-glucose-deprivation/reoxygenation (OGD/R) group at 0.5 and 2 h of reoxygenation; the formation of autophagosomes containing cell fractions is observed. (g) Autophagosome formation and fusion of autophagosomes to lysosomes to form autolysosomes are observed in the JNK inhibitor pretreatment + OGD/R group at 6h of reoxygenation. (h) A large number of empty autophagosomes is observed, whereas few newly formed autophagosomes are detected in the JNK inhibitor pretreatment + OGD/R group at 12 h of reoxygenation (Data was not shown) (Scale bar = 1 μm; single arrow indicates autophagosomes, autolysosomes or empty autophagic vacuoles; double arrows indicate mitochondria).

such as mitochondria and endoplasmic reticulum showed normal morphology, without mitochondrial swelling, crista disorder or reduction, endoplasmic reticulum swelling or

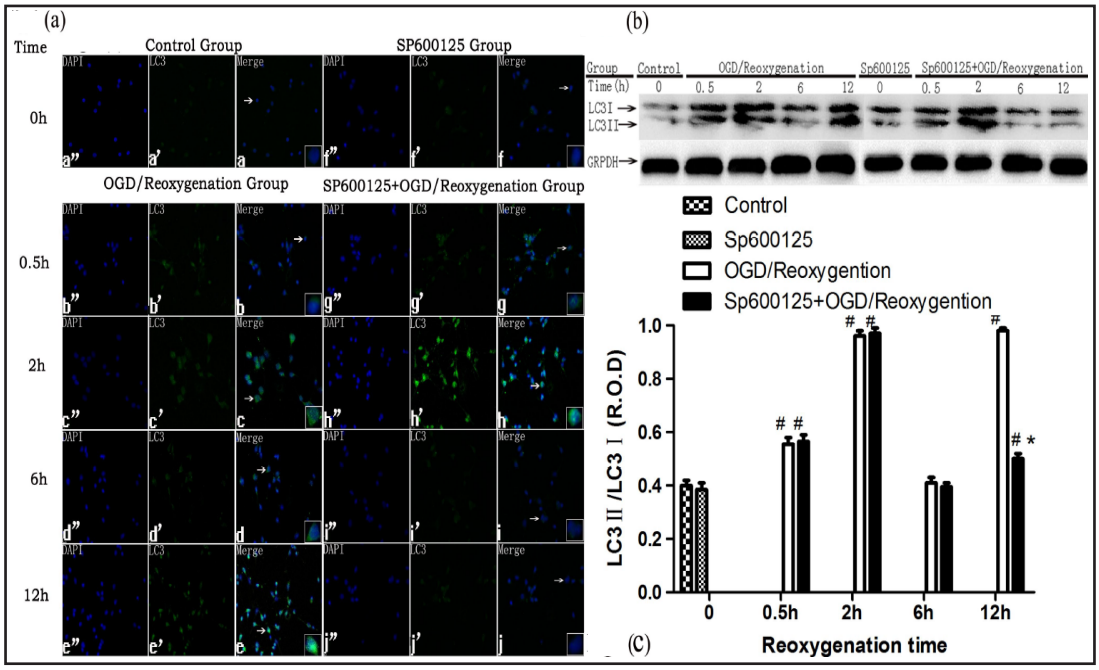

Fig. 4. Immunofluorescence and western blot detection of LC3 expression. (A) Immunofluorescence analysis showed extremely low LC3 expression in the blank control group (a), gradual increases in the neurons positive for LC3 and a significant increase in LC3 expression in the cytoplasm in the experimental group at 0.5 (b) and 2h of reoxygenation (c). LC3 expression decreased slightly at 6h (d) and increased rapidly at 12h (e). LC3 expression was almost undetectable in the JNK inhibitor treatment group (f). The amount of granular LC3 increased significantly at 0.5 (g) and 2h of reoxygenation (h) in the JNK inhibitor pretreatment + OGD/R group, and decreased at 6 (i) and 12 h (j). (B) and (C) Western blot analysis showed that LC3II expression followed an increase/decrease pattern in the experimental group and the JNK inhibitor pretreatment + OGD/R group at 0.5, 2 and 6h of reoxygenation and was higher in the JNK inhibitor pretreatment + OGD/R group. LC3II expression showed a rapid increase at 12 h of reoxygenation in the experimental group, whereas it remained low in the JNK inhibitor pretreatment + OGD/R group (# $P < 0.05$, experimental group vs. control group, and JNK inhibitor pretreatment + OGD/R group vs. JNK inhibitor treatment group; * $P < 0.05$, JNK inhibitor pretreatment + OGD/R group vs. experimental group) (*200).

extension. After 6 h of reoxygenation, autophagic vacuoles fused with lysosomes forming autolysosomes with single-layer membrane structures characteristic of the preliminary binding of autophagosomes to lysosomes, and the gradual degradation of cytoplasmic components or cell fractions within the autolysosome was observed. In addition, a large number of phagophores appeared in the plasma of neurons. After 12 h of reoxygenation, severe nuclear pyknosis and chromatin margination were observed, and the condensation of the cytoplasm induced aggregation of organelles (mitochondria and endoplasmic reticulum). Hydrolyzation of the contents of autolysosomes resulted in the appearance of vacuoles, and a large number of new autophagosomes containing mitochondria, endoplasmic reticulum and ribosomes were observed. The neuronal soma was not plump in the JNK inhibitor treatment group and the nuclear membrane and plasma membrane showed slight shrinking; however, no cellular damage was observed. The appearance of autophagosomes and autolysosomes was correlated with reoxygenation time in the JNK inhibitor pretreatment + OGD/R group, although with significantly lower numbers than in the experimental group. These results indicated that neuronal viability declined and increased with reoxygenation time in the experimental group, and autophagosome formation decreased with increasing reoxygenation time in the JNK inhibitor treatment group.

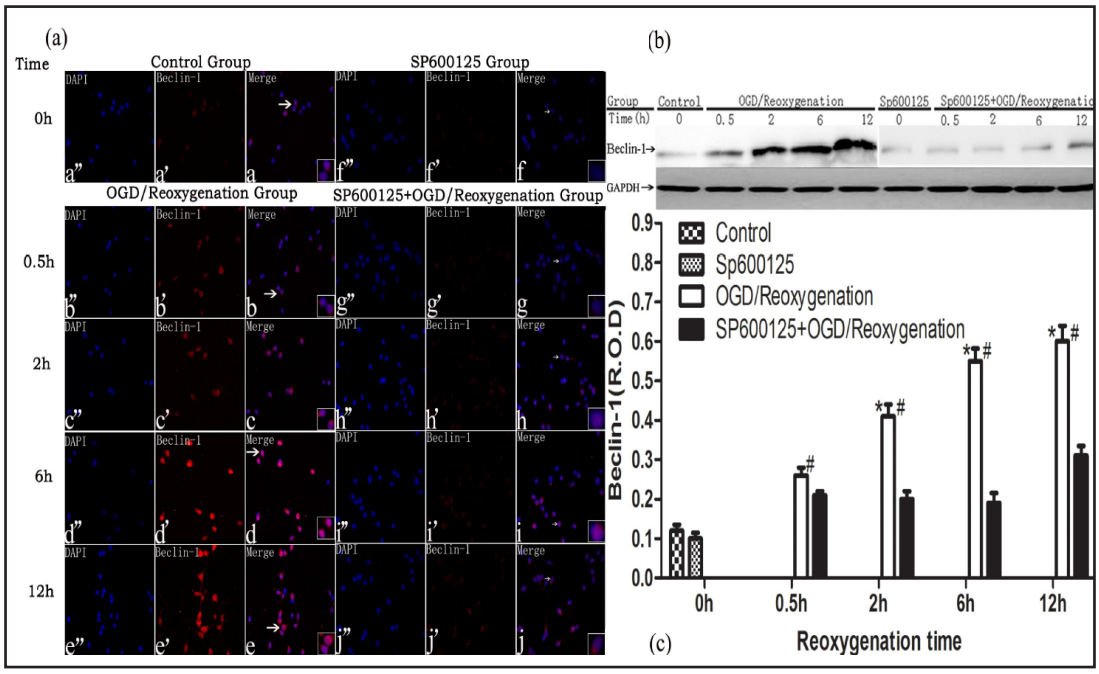

Fig. 5. Immunofluorescence and western blot detection of Beclin-1 expression. (A) Immunofluorescence analysis showed extremely low Beclin-1 expression in the blank control group (a) and the JNK inhibitor treatment group (e). The number of Beclin-1 positive neurons and the intensity of Beclin-1 staining increased gradually in the experimental group at 0.5 (b), 2 (c), 6 (d) and 12 h (e) of reoxygenation. No apparent changes in Beclin-1 expression were detected in the JNK inhibitor pretreatment + oxygen-glucose-deprivation/reoxygenation (OGD/R) group at 0.5 (f), 2 (h) and 6 h (i) of reoxygenation, although Beclin-1 expression increased after 12 h (j). (B) Western blot analysis showed a gradual increase in Beclin-1 expression in the experimental group, which was suppressed by the JNK inhibitor until after 12 h of reoxygenation ($P < 0.05$) (# $P < 0.05$, experimental group vs. control group, and JNK inhibitor pretreatment + OGD/R group vs. JNK inhibitor treatment group; * $P < 0.05$, JNK inhibitor pretreatment + OGD/R group vs. experimental group) (*200).

Immunofluorescence and western blot detection of LC3 expression

LC3 plays an important role in the formation of autophagic vacuoles, and LC3II specifically localizes to the double-layer membrane of the autophagosome. Therefore, immunofluorescence detection of LC3 was used to verify autophagosome formation. LC3 expression was barely detectable in the blank control and JNK inhibitor treatment groups. In the experimental group, LC3 positive neurons increased gradually at 0.5 h and 2 h, and decreased at 6 h, 12 h of reoxygenation. The JNK inhibitor pretreatment + OGD/R group showed a similar pattern of increase-decrease of LC3 expression at 0.5, 2 and 6 h of reoxygenation, with a more intense staining pattern than that of the experimental group; however, unlike the experimental group, the number of LC3 positive neurons increased in this group at 12 h of reoxygenation. Western blot analysis confirmed the increase-decrease pattern of LC3II expression in the experimental group and the JNK inhibitor pretreatment + OGD/R group at 0.5, 2 and 6 h of reoxygenation, as well as the higher level of expression in the JNK inhibitor pretreatment + OGD/R group. LC3II expression increased rapidly at 12 h in the experimental group whereas it decreased in the JNK inhibitor treatment group. LC3 expression as a marker of autophagosome formation confirmed the electron microscopic findings showing that autophagosome formation decreased and increased with reoxygenation time in the experimental group and autophagosome formation was reduced in the JNK inhibitor pretreatment + OGD/R group.

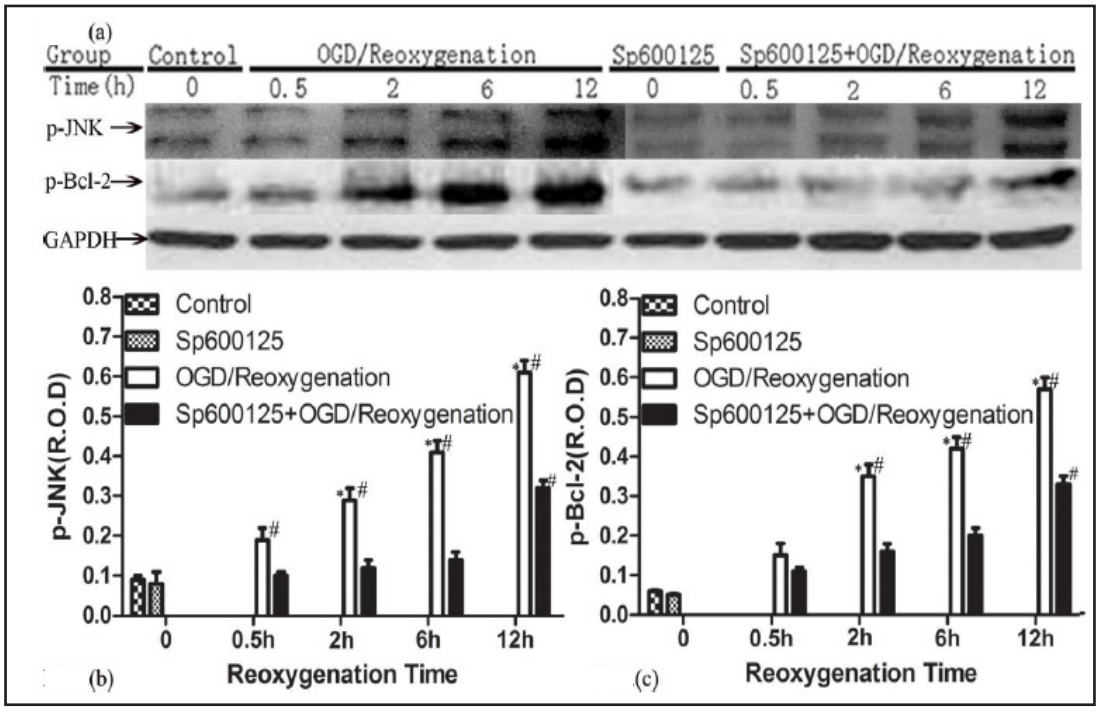

Fig. 6. Western blot analysis showed a gradual increase in the level of phosphorylated JNK with increasing reoxygenation time in the experimental group, which is suppressed in the JNK inhibitor pretreatment + oxygen-glucose-deprivation/reoxygenation (OGD/R) group until 12 h after reoxygenation ($P < 0.05$). In parallel with the changes in the level of phosphorylated JNK, the expression of phosphorylated Bcl-2 (ser70) increased gradually in the experimental group, whereas only a slight increase in the level of phosphorylated Bcl-2 was detected in the JNK inhibitor pretreatment + OGD/R group after 12 h of reoxygenation ($P < 0.05$) (# $P < 0.05$, experimental group vs. control group, and JNK inhibitor pretreatment + OGD/R group vs. JNK inhibitor treatment group; * $P < 0.05$, JNK inhibitor pretreatment + OGD/R group vs. experimental group).

Immunofluorescence and western blot detection of Beclin-1 expression

Beclin-1 plays an important role in autophagosome formation and it is therefore considered as a marker for the activation of autophagosomes. Immunofluorescence analysis showed a gradual increase in the number of Beclin-1 positive neurons and staining intensity in correlation with reoxygenation time in the experimental group. However, in the JNK inhibitor pretreatment + OGD/R group, Beclin-1 expression did not increase until after 12 h of reoxygenation. Western blot analysis confirmed that Beclin-1 expression increased gradually in the experimental group, and this increase was suppressed by JNK inhibitor treatment, with the inhibitory effect decreasing gradually until 12 h of reoxygenation ($P < 0.05$).

Determination of JNK activity and Bcl-2 expression

JNK is a cytoplasmic serine/threonine protein kinase that is activated by extracellular stress factors and phosphorylated at Thr 83 and Tyr 85, triggering the downstream phosphorylation of Bcl-2. Therefore, we analyzed the expression of phosphorylated JNK (Thr 83/Tyr 85) and Bcl-2 (ser70). Our results showed that the level of phosphorylated JNK increased gradually with reoxygenation time in the experimental group, and this effect was suppressed in the JNK inhibitor pretreatment + OGD/R group, which showed a slight increase in phosphorylated JNK at 12 h of reoxygenation ($P < 0.05$). In a similar pattern, the level of phosphorylated Bcl-2 (ser70) increased gradually in the experimental group and showed a slight increase in the JNK inhibitor pretreatment + OGD/R group after 12 h of reoxygenation ($P < 0.05$). These results indicated that JNK and Bcl-2 were activated in the experimental

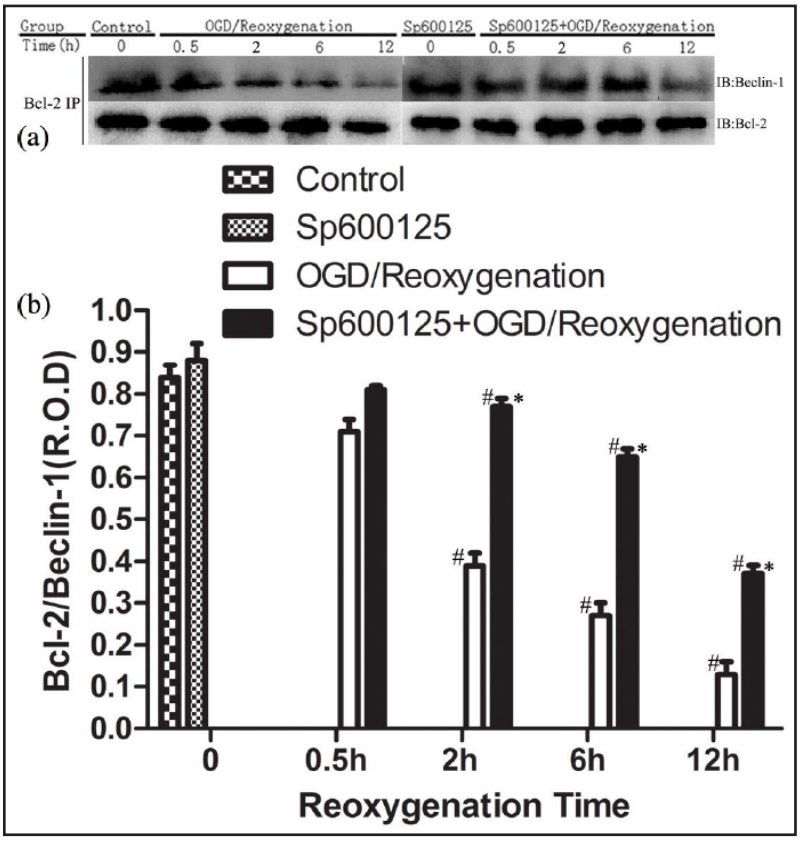

Fig. 7. Beclin-1/Bcl-2 co-immunoprecipitation assay showed the gradual dissociation of the Bcl-2/Beclin-1 complex in correlation with increased reoxygenation time in the experimental group, while a relatively stable Bcl-2/Beclin-1 complex was observed in the JNK inhibitor pretreatment + oxygen-glucose-deprivation/reoxygenation (OGD/R) group, and partial dissociation was detected at 12 h of reoxygenation ($P < 0.05$) (# $P < 0.05$, experimental group vs. control group, and JNK inhibitor pretreatment + OGD/R group vs. JNK inhibitor treatment group; * $P < 0.05$, JNK inhibitor pretreatment + OGD/R group vs. experimental group).

group, and JNK activity and Bcl-2 expression increased with increasing reoxygenation time, while this effect was suppressed by JNK inhibitor treatment.

Interaction between Beclin-1 and Bcl-2

Beclin-1, which contains a BH3 domain, can selectively and stably bind to the pro-apoptotic protein Bcl-2 via its hydrophobic groove under physiological conditions. However, Beclin-1 dissociates from Bcl-2 in response to external stimuli and regulates cellular processes including autophagosome formation. Our results showed the gradual dissociation of the Bcl-2/Beclin-1 complex during reoxygenation in the experimental group. On the other hand, a relatively stable Bcl-2/Beclin-1 complex was observed in the JNK inhibitor pretreatment + OGD/R group, with slight complex dissociation detected after 12 h of reoxygenation. These results suggested that in the experimental group, reoxygenation caused the gradual dissociation of Beclin-1 from Bcl-2 and therefore its activation, whereas in the JNK inhibitor pretreatment + OGD/R group, Beclin-1 was activated after 12 h of reoxygenation.

Discussion

Ischemia/reperfusion injury is frequently associated with neuronal damage and hypoxia is a known stimulus of autophagy [21]. The OGD/R *in vitro* experimental model is a widely accepted and used model for simulating *in vivo* ischemia/reperfusion injury. In the past few decades, the relationship between apoptosis and autophagy-related cell death had attracted increasing attention in many fields of biological science [22]. The underlying mechanism of neuronal injury during ischemia/reperfusion is thought to involve necrosis (type III cell death) and apoptosis (type I cell death). In the present study, we show that autophagic cell death (type II cell death) is involved in neuronal damage associated with ischemia/reperfusion injury. The morphology and biochemical pathways of autophagy are

significantly different from those of apoptosis and necrosis; however, the activities of these three forms of cell death are related. Activation of autophagy during the early phases of injury protects cells from death and alleviates necrosis and apoptosis-induced cell damage, whereas autophagy triggered during the late phases of injury functions in association with necrosis and apoptosis to promote cell death [23]. As shown in Fig. 2, the results of the MTT assay showed a non-linear decrease in neuronal viability in response to reoxygenation in the experimental group, with 69% of surviving neurons in the blank control group at 2h and 13% at 12 h of reoxygenation. Furthermore, mild neuronal injury was detected at the early phase of OGD/R, whereas it was severe in the late phase. In Fig. 3, a large number of autophagic vacuoles were detected by electron microscopy at 2 and 12h of reoxygenation. In addition, as shown in Fig. 4, western blotting and immunofluorescence showed two peaks of LC3II expression at 2 and 12h of reoxygenation. Taken together, these results suggest that autophagy is activated twice at 2 and 12h of reoxygenation and may play different roles during these two periods. Autophagy has been shown to play distinct roles during ischemia and reperfusion, having a protective function during the ischemia phase, and a role in tissue damage during the reperfusion phase [24]. Therefore, the autophagic flux activated at the initial phase of reoxygenation (0.5 and 2 h) in our study may have a protective function in neurons, while the autophagy triggered at the late phase of reoxygenation (12h) may be associated with cell death.

In the current study, neuronal viability decreased slowly in the JNK inhibitor pretreatment + OGD/R group, with 41% of surviving neurons observed at 12h of reoxygenation. In addition, a significant number of autophagosomes was observed at 2h, and the autophagic flux was not present at 12h. LC3II expression increased at the initial phase of reoxygenation (0.5 and 2h), but declined at the late phase of reoxygenation (6 and 12h), suggesting that the JNK inhibitor suppressed autophagic cell death, but did not affect the formation of protective autophagosomes. The JNK inhibitor SP600125 has been shown to inhibit brain ischemia/reperfusion-induced neuronal death in the rat hippocampus via nuclear and non-nuclear pathways [25]. Activated JNK translocates to mitochondrial membranes and modulates the pro-apoptotic activity of Bcl-2 family proteins [14]. Our previous study showed that SP600125 inhibited JNK activity, thereby inhibiting the dissociation of BAD and 14-3-3 and alleviating ischemia and reperfusion-induced spinal cord injury [16]. Unlike pro-apoptotic proteins such as BAD, the anti-apoptotic protein Bcl-2 contains all four Bcl-2 homology (BH) domains (BH1–BH4). Bcl-2 binds to pro-apoptotic proteins and forms stable complexes that reduce their pro-apoptotic effect. Although the role of Bcl-2 phosphorylation in the regulation of apoptosis remains controversial, it has been shown to reduce its anti-apoptotic effect [26]. Four phosphorylation sites have been identified within Bcl-2 including Thr56, Ser70, Thr74, and Ser87, and Ser70 phosphorylation is associated with JNK-induced apoptosis [27, 28]. JNK activation by phosphorylation significantly promotes Bcl-2 phosphorylation, enabling the release of pro-apoptotic proteins bound to Bcl-2 and promoting cell death [29]. In models of excitotoxicity and ischemia, cell death is accompanied by the activation of autophagy and the down-regulation of the anti-apoptotic protein Bcl-2, and these effects are suppressed by autophagy inhibitors, suggesting that Bcl-2 mediates apoptosis and is involved in the modulation of autophagic cell death [30]. Beclin 1 is a key regulatory protein that contains a BH3 domain and is therefore classified into the third class of Bcl-2 proteins together with other pro-apoptotic and anti-apoptotic BH3-only proteins. Beclin-1 binds to the anti-apoptotic proteins Bcl-2 or Bcl-xl through its central coiled-coil domain and its interaction with Bcl-2 inhibits acute starvation-induced autophagy [13]. In the Fig. 6 and Fig. 7, we showed that OGD/R activates JNK, promoting the phosphorylation and activation of Bcl-2 (Ser70) and its dissociation from Beclin-1, resulting in the release of Beclin-1. Beclin-1-mediated autophagy has been shown to cause tissue damage in the heart during ischemia and reperfusion. Our findings showed that the upregulation of Beclin-1 expression promoted the formation of autophagosomes and consequently decreased neuronal viability (Fig. 5). Increased levels of phosphorylated JNK and Bcl-2, dissociation of the Bcl-2/Beclin-1 complex, and increased Beclin-1 expression were not observed in the JNK inhibitor

pretreatment + OGD/R group until 6h after reoxygenation, suggesting that the inhibition of JNK phosphorylation by SP600125 protected the activity of Bcl-2 and the integrity of the Bcl-2/Beclin-1 complex, thus reducing Beclin-1-mediated autophagic cell death.

Bcl-2, however, does not inhibit the activation of autophagy under any conditions. Ischemia induces autophagy in HeLa cells overexpressing Bcl-2 and Bcl-xl [31]. Therefore, further studies are necessary to evaluate the association between Bcl-2 and autophagy. Zhang F et al. confirmed that hypoxia promoted autophagy via depressing Bcl-2 [32]. However, the present study showed that autophagic cell death is responsible for the decrease in neuronal viability at the late phase of OGD/R injury, and this process is associated with JNK activation, phosphorylation and inactivation of Bcl-2, and the dissociation of the Bcl-2/Beclin-1 complex. Our findings indicate that autophagy plays a dual role in OGD/R injury by promoting both neuronal survival and death, and the JNK/Bcl-2/Beclin-1 signaling pathway is involved in the modulation of autophagic cell death. Further studies will be aimed at investigating the mechanisms underlying autophagic cell death in animal models of ischemia-reperfusion injury. In addition, the association between the up-regulation of autophagy and the nuclear translocation of Bcl-2, and the role of posttranslational modifications of Bcl-2 in the regulation of autophagy should be addressed in future studies.

Acknowledgments

This work was supported by National Natural and Science Foundation (81371967, 81401807).

Disclosure Statement

The authors declare that they have no conflict of interest.

References

1 Komatsu M, Waguri S, Ueno T, Iwata J, Murata S, Tanida I, Ezaki J, Mizushima N, Ohsumi Y, Uchiyama Y, Kominami E, Tanaka K, Chiba T: Impairment of starvation-induced and constitutive autophagy in Atg7-deficient mice. J Cell Biol 2005;169:425-434.
2 Kuma A, Hatano M, Matsui M, Yamamoto A, Nakaya H, Yoshimori T, Ohsumi Y, Tokuhisa T, Mizushima N: The role of autophagy during the early neonatal starvation period. Nature 2004;432:1032-1036.
3 Deretic V, Levine B: Autophagy, immunity, and microbial adaptations. Cell Host Microbe 2009;5:527-549.
4 Deretic V: Links between autophagy, innate immunity, inflammation and Crohn's disease. Dig Dis 2009;27:246-251.
5 Adams JM: Ways of dying: multiple pathways to apoptosis. Genes Dev 2003;17:2481-2495.
6 Kabeya Y, Mizushima N, Ueno T, Yamamoto A, Kirisako T, Noda T, Kominami E, Ohsumi Y, Yoshimori T: LC3, a mammalian homologue of yeast Apg8p, is localized in autophagosome membranes after processing. EMBO J 2000;19:5720-5728.
7 Yue Z, Jin S, Yang C, Levine AJ, Heintz N: Beclin 1, an autophagy gene essential for early embryonic development, is a haploinsufficient tumor suppressor. Proc Natl Acad Sci USA 2003;100:15077-15082.
8 Zeng X, Overmeyer JH, Maltese WA: Functional specificity of the mammalian Beclin-Vps34 PI 3-kinase complex in macroautophagy versus endocytosis and lysosomal enzyme trafficking. J Cell Sci 2006;119:259-270.
9 Oberstein A, Jeffrey PD, Shi Y: Crystal structure of the Bcl-XL-Beclin 1 peptide complex: Beclin 1 is a novel BH3-only protein. J Biol Chem 2007;282:13123-13132.
10 Liang XH, Kleeman LK, Jiang HH, Gordon G, Goldman JE, Berry G, Herman B, Levine B: Protection against fatal Sindbis virus encephalitis by beclin, a novel Bcl-2-interacting protein. J Virol 1998;72:8586-8596.
11 Walensky LD: BCL-2 in the crosshairs: tipping the balance of life and death. Cell Death Differ 2006;13:1339-1350.
12 Youle RJ, Strasser A: The BCL-2 protein family: opposing activities that mediate cell death. Nat Rev Mol Cell Biol 2008;9:47-59.

13 Wei Y, Pattingre S, Sinha S, Bassik M, Levine B: JNK1-mediated phosphorylation of Bcl-2 regulates starvation-induced autophagy. Mol Cell 2008;30:678-688.
14 Kharbanda S, Saxena S, Yoshida K, Pandey P, Kaneki M, Wang Q, Cheng K, Chen YN, Campbell A, Sudha T, Yuan ZM, Narula J, Weichselbaum R, Nalin C, Kufe D: Translocation of SAPK/JNK to mitochondria and interaction with Bcl-x(L) in response to DNA damage. J Biol Chem 2000;275:322-327.
15 Lin A: Activation of the JNK signaling pathway: breaking the brake on apoptosis. Bioessays 2003;25:17-24.
16 Fan J, Xu G, Nagel DJ, Hua Z, Zhang N, Yin G: A model of ischemia and reperfusion increases JNK activity, inhibits the association of BAD and 14-3-3, and induces apoptosis of rabbit spinal neurocytes. Neurosci Lett 2010;473:196-201.
17 Takei N, Numakawa T, Kozaki S, Sakai N, Endo Y, Takahashi M, Hatanaka H: Brain-derived neurotrophic factor induces rapid and transient release of glutamate through the non-exocytotic pathway from cortical neurons. J Biol Chem 1998;273:27620-27624.
18 Goldberg MP, Choi DW: Combined oxygen and glucose deprivation in cortical cell culture: calcium-dependent and calcium-independent mechanisms of neuronal injury. J Neurosci 1993;13:3510-3524.
19 Chen T, Liu W, Chao X, Qu Y, Zhang L, Luo P, Xie K, Huo J, Fei Z: Neuroprotective effect of osthole against oxygen and glucose deprivation in rat cortical neurons: involvement of mitogen-activated protein kinase pathway. Neuroscience 2011;183:203-211.
20 Berridge MV, Tan AS: Characterization of the cellular reduction of 3-(4,5-dimethylthiazol-2-yl)-2,5-diphenyltetrazolium bromide (MTT): subcellular localization, substrate dependence, and involvement of mitochondrial electron transport in MTT reduction. Arch Biochem Biophys 1993;303:474-482.
21 Wu J, Niu J, Li X, Li Y, Wang X, Lin J, Zhang F: Hypoxia induces autophagy of bone marrow-derived mesenchymal stem cells via activation of ERK1/2. Cell Physiol Biochem 2014;33:1467-1474.
22 Wang XM, Yang YJ, Wu YJ, Zhang Q, Qian HY: Attenuating Hypoxia-Induced Apoptosis and Autophagy of Mesenchymal Stem Cells: the Potential of Sitagliptin in Stem Cell-Based Therapy. Cell Physiol Biochem 2015;37:1914-1926.
23 Oh S, Xiaofei E, Ni D, Pirooz SD, Lee JY, Lee D, Zhao Z, Lee S, Lee H, Ku B, Kowalik T, Martin SE, Oh BH, Jung JU, Liang C: Downregulation of autophagy by Bcl-2 promotes MCF7 breast cancer cell growth independent of its inhibition of apoptosis. Cell Death Differ 2011;18:452-464.
24 Matsui Y, Takagi H, Qu X, Abdellatif M, Sakoda H, Asano T, Levine B, Sadoshima J: Distinct roles of autophagy in the heart during ischemia and reperfusion: roles of AMP-activated protein kinase and Beclin 1 in mediating autophagy. Circ Res 2007;100:914-922.
25 Guan QH, Pei DS, Zhang QG, Hao ZB, Xu TL, Zhang GY: The neuroprotective action of SP600125, a new inhibitor of JNK, on transient brain ischemia/reperfusion-induced neuronal death in rat hippocampal CA1 via nuclear and non-nuclear pathways. Brain Res 2005;1035:51-59.
26 Bassik MC, Scorrano L, Oakes SA, Pozzan T, Korsmeyer SJ: Phosphorylation of BCL-2 regulates ER Ca2+ homeostasis and apoptosis. EMBO J 2004;23:1207-1216.
27 Maundrell K, Antonsson B, Magnenat E, Camps M, Muda M, Chabert C, Gillieron C, Boschert U, Vial-Knecht E, Martinou JC, Arkinstall S: Bcl-2 undergoes phosphorylation by c-Jun N-terminal kinase/stress-activated protein kinases in the presence of the constitutively active GTP-binding protein Rac1. J Biol Chem 1997;272:25238-25242.
28 Deng X, Xiao L, Lang W, Gao F, Ruvolo P, May WS, Jr: Novel role for JNK as a stress-activated Bcl2 kinase. J Biol Chem 2001;276:23681-23688.
29 Lei K, Davis RJ: JNK phosphorylation of Bim-related members of the Bcl2 family induces Bax-dependent apoptosis. Proc Natl Acad Sci USA 2003;100:2432-2437.
30 Wen YD, Sheng R, Zhang LS, Han R, Zhang X, Zhang XD, Han F, Fukunaga K, Qin ZH: Neuronal injury in rat model of permanent focal cerebral ischemia is associated with activation of autophagic and lysosomal pathways. Autophagy 2008;4:762-769.
31 Degenhardt K, Mathew R, Beaudoin B, Bray K, Anderson D, Chen G, Mukherjee C, Shi Y, Gelinas C, Fan Y, Nelson DA, Jin S, White E: Autophagy promotes tumor cell survival and restricts necrosis, inflammation, and tumorigenesis. Cancer Cell 2006;10:51-64.
32 Zhang F, Wang J, Chu J, Yang C, Xiao H, Zhao C, Sun Z, Gao X, Chen G, Han Z, Zou W, Liu T: MicroRNA-146a Induced by Hypoxia Promotes Chondrocyte Autophagy through Bcl-2. Cell Physiol Biochem 2015;37:1442-1453.